Nanoparticle Sensors

DOI: 10.1002/anie.200804231

Europium-Based Fluorescence Nanoparticle Sensor for Rapid and Ultrasensitive Detection of an Anthrax Biomarker**

*Kelong Ai, Baohua Zhang, and Lehui Lu**

During the past decade the threat of biological attack with *B. anthracis* spores, a potential biological warfare agent, has been of particular concern throughout the word.[1,2] Inhalation of more than 10^4 *B. anthracis* spores can lead to death unless medical attention is received within 24–48 h.[3] Therefore, the rapid and ultrasensitive detection of *B. anthracis* spores prior to infection is critical for the prevention and control of anthrax disease or bioterrorism.

Lanthanide-based sensors have gained a great deal of attention in recent years owing to their unique spectroscopic characteristics, including long fluorescence lifetime, large Stoke shift, and sharp line-like emission bands.[4,5] These properties are particularly attractive because they enable temporal and spectral discrimination against background fluorescence often associated with commonly used fluorophores in chemical biology, leading to excellent detection sensitivity. To date, terbium has been considered as the best lanthanide for the detection of *B. anthracis* spores because of its bright fluorescence, long fluorescence lifetime, and high enhancement ratio.[1b,c,f,5b,6] To our knowledge, the use of europium(III) for fluorescent sensing of *B. anthracis* spores has not been achieved. This is probably based on the general belief that excited states of Eu^{III} can couple more efficiently with the high-frequency OH oscillators of water molecules than Tb^{III}, resulting in enhancement of nonradiative quenching of the Eu^{III} emission and hence lower detection sensitivity.[7] Nevertheless, Eu^{III} offers several advantages over Tb^{III} in terms of larger Stoke shift, a red emission, and exclusion of second-order scattering interference in the maximum fluorescence intensity. These advantages apply particularly to the case of a nanoparticle sensor, which is very desirable for applications in complex environments, such as those found in spores. More importantly, false-positive results arising from the nonselective binding of aromatic compounds to Tb^{III} can be decreased with the europium-based sensor, as discussed below. Hence, the quest to prepare europium-based sensors with rapid response, high sensitivity, and improved selectivity is of great importance.

Herein, we present the first example of a europium-based fluorescence nanoparticle sensor for rapid and ultrasensitive detection of *B. anthracis* spores in aqueous solution. By grafting the sensing moiety (Eu^{III} complex) onto the surface of organic-dye-doped silica nanoparticles, a nanoparticle sensor with optimal geometry is produced, which sequesters the reference dye in the core while offering the greatest possible surface area for sensing of *B. anthracis* spores. Several features of such a sensor make it particularly attractive for the detection of *B. anthracis* spores: 1) the stabilization through covalent bonding of both the reference dye and the sensing moiety minimizes their leaching thus giving a stable sensor with low background signal and enabling quantitative chemical sensing down to the single nanoparticle level; 2) incorporation of the reference dye as a non-interfering internal calibration makes it possible for use as a ratiometric sensor; 3) this architecture can improve the thermal stability and mechanical properties of the sensing moiety, enabling practical applications, and allowing the sensing moiety to be separated from the analyte solution.

B. anthracis spores can be identified through the detection of calcium dipicolinate (CaDPA), a unique biomarker for bacillus spores, which accounts for about 10% of the spore dry weight and is not found in other common spores, such as pollen or mold.[1b,f] With this novel sensor, a procedure taking only 2 min is capable of achieving a limit of detection (LOD) of 0.2 nM CaDPA, which is approximately six orders-of-magnitude lower than an infectious dosage of the spores and is two orders-of-magnitude better than those reported using $TbCl_3$ as a sensor reagent.[1b,c]

Our strategy for the fabrication of a europium-based fluorescence nanoparticles sensor is outlined in Scheme 1. In the first step, uniform fluorescein isothiocyanate (FITC) dye-doped silica nanoparticles are prepared using a reverse microemulsion method and subsequently modified with 3-aminopropyltriethoxysilane (APTES).[8] With this synthesis approach, FITC with high quantum yield ($\Phi = 0.93$), as a reference dye, is protected from external influences such as solvents, providing a stable reference signal. Next, ethylenediamine tetraacetic acid dianhydride (EDTAD) is synthesized according to the procedure published by Paik et al.[9] and then covalently grafted onto the surface of the FITC-doped silica nanoparticles by the reaction of the amino group present on the APTES molecules with the anhydride group of EDTAD molecules. The resulting EDTA ligand is then readily converted into a $[Eu(EDTA)(H_2O)_3]$ complex on reaction with $EuCl_3$ (Sensor 1). Upon exposure of Sensor 1 to CaDPA, water molecules are excluded from the Eu^{III}

[*] K. L. Ai, B. H. Zhang, Prof. L. H. Lu
State Key Laboratory of Electroanalytical Chemistry Changchun Institute of Applied Chemistry
Chinese Academy of Sciences
5625 Renmin Street, Changchun 130022 (P.R. China)
Fax: (+86) 431-8526-2406
E-mail: lehuilu@ciac.jl.cn

[**] Financial support by the "Hundred Talents Project" (Initialization Support) of the Chinese Academy of Sciences, the National Natural Science Foundation of China (No. 20873138; No. 20845001), and the Program for Excellent Doctoral Thesis of Chinese Academy of Sciences is gratefully acknowledged.

Supporting information for this article is available on the WWW under http://dx.doi.org/10.1002/anie.200804231.

InterScience DISCOVER SOMETHING GREAT
© 2009 Wiley-VCH Verlag GmbH & Co. KGaA, Weinheim

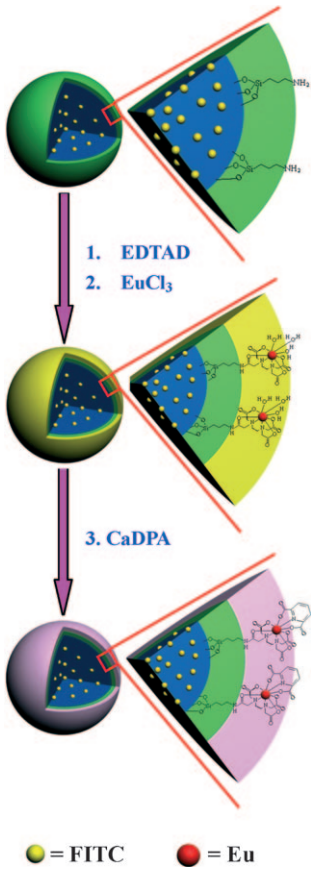

Scheme 1. Design strategy for europium-based fluorescence nanoparticle sensor, see text for details.

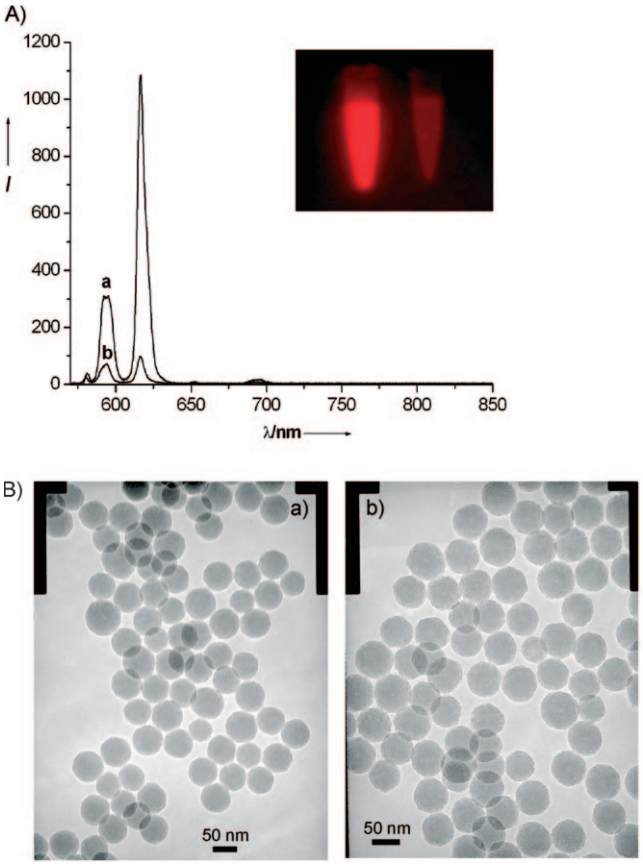

Figure 1. A) Fluorescence spectra of a) Sensor 1 and b) Sensor 2 in the presence of 1 μM CaDPA at pH 6.5. The inset shows visual fluorescence color of Sensor 1 (left) and Sensor 2 (right) in the presence of 10 μM CaDPA (filtration with a CB565 filter). B) TEM images of FITC-doped silica nanoparticles a) without and b) with the sensing moiety.

coordination sphere through to the formation of [Eu(EDTA)-(DPA)] complex, which significantly minimizes the non-radiative quenching of the Eu^{III} emission, resulting in an increase in the overall quantum yield and thereby affording a corresponding improvement in the detection sensitivity for CaDPA.

As a proof of this strategy, we compared fluorescence spectra of Sensor 1 and the free $EuCl_3$ sensor agent (Sensor 2) in the presence of 1 μM CaDPA, as illustrated in Figure 1 A. Both Sensor 1 and Sensor 2 in aqueous solution were non-fluorescent upon excitation at 270 nm. Upon exposure to CaDPA, Eu^{III} emission in both cases was evident from the appearance of line-like emission bands at 580, 594, and 616 nm, respectively, corresponding to the deactivation of the Eu^{III} excited states $^5D_0 \rightarrow {}^7F_J$ ($J = 0$, 1, and 2).[7] However, it was clear that Sensor 1 exhibited the highest fluorescent enhancement efficiency, which was readily visible to the naked eye under a UV-lamp (taken after filtration with a CB565 filter). The fluorescent quantum yield (Φ) was calculated to be up to 0.15 by using $[Ru(bpy)_3Cl_2]$ (bpy = bipyridine) as a reference,[1f] a value which was 38-fold higher than that of Sensor 2 ($\Phi = 0.004$). As stated above, Eu^{III} complexes containing coordinating water molecules often exhibit low luminescence yields because of enhanced non-radiative quenching resulting from the efficient vibronic coupling of the $^5D_0$ excited states with the high-frequency OH oscillators.[7] Nevertheless, an increase in the overall quantum yield can be achieved by displacing such water molecules with appropriate ligands, such as EDTA and DOTA (1,4,7,10-tetraazacyclododecane-1,4,7,10-tetraacetic acid).[5a,b] To verify that this was the case for Sensor 1 and Sensor 2, the coordination geometry of the Eu^{III} centers was evaluated in aqueous solution by determining the number of coordinating water molecules (q) of the Eu^{III} complexes by measuring their excited state lifetimes (τ) in H_2O and D_2O (Supporting Information, Figure S3). The values for Sensor 1 and Sensor 2 was determined to be approximately 0 and 6, respectively (Sensor 1: $\tau_{H_2O} = 1.2$ ms, $\tau_{D_2O} = 2.3$ ms, $q = 0.4$; Sensor 2: $\tau_{H_2O} = 0.2$ ms, $\tau_{D_2O} = 3.0$ ms, $q = 5.7$), indicating that the Eu^{III} complex with CaDPA in Sensor 1, [Eu(EDTA)(DPA)], retains its ligands in aqueous solution, while the Eu^{III} complex with CaDPA in Sensor 2 contains six coordinating water molecules, $[Eu(H_2O)_6(DPA)]$. These results strongly support the reliability of our proposed strategy for the construction of europium-based fluorescence nanoparticles sensor for anthrax biomarker CaDPA.

Of particular importance for this strategy is the generation of high-quality FITC-doped silica nanoparticles. In this case, we developed a facile method to achieve this aim. The main idea of the synthesis comes from the results of Ref. [8a] A

 © 2009 Wiley-VCH Verlag GmbH & Co. KGaA, Weinheim

complex of FITC and APTES was prepared directly in 1-hexanol and then added to the mixture of Triton X-100, 1-hexanole, cyclohexane, and water. Subsequent polycondensation of tetraethoxysilane (TEOS) leads to the formation of FITC-doped silica nanoparticles. The average diameter of these nanoparticles is (63 ± 3) nm, as characterized by transmission electron microscopy (TEM, Figure 1 B a). The size can be tuned by changing experimental conditions. After grafting the sensing moiety onto the nanoparticles, TEM analysis showed spherical nanoparticles with a rough surface and an average diameter of (65 ± 3) nm and no evidence of aggregation (Figure 1 B b).

To evaluate the sensitivity of this sensor, fluorescence titrations were conducted in the presence of an excess of Sensor 1 (Eu^{III} content: 10 μM). As seen in Figure 2 A, the intensity of the fluorescence emission of Sensor 1 was highly sensitive to CaDPA and increased upon addition of increasing concentration of CaDPA, whereas no fluorescence change was observed for reference dye FITC, even at high concentrations of CaDPA (Supporting Information, Figure S4). The hypersensitive $\Delta J = 2$, centered at 616 nm, gave rise to the greatest changes in the Eu^{III} emission, revealing the direct coordination of CaDPA to the Eu^{III} center and the displacement of three coordinating water molecules from the Eu^{III} center.[7,10] A linear correlation existed between the maximum emission intensity at 616 nm and the concentration of CaDPA over the range from 0.6 nM to 600 nM ($R^2 = 0.99$; Figure 2 B). The LOD value for CaDPA, at a signal-to-noise (S/N) ratio of 3, was 0.2 nM, which is six-orders-of magnitude lower than an infectious dosage of the spores (6×10^{-5} M required).[1b,c,2c] This strategy provides a sensitivity that is about two orders of magnitude better than the previously reported those by using $TbCl_3$ as sensor reagent,[1b,c] and comparable to the terbium-based metal–organic nanosensors.[6] Interestingly, the CaDPA sensing and the concomitant fluorescent changes were clearly visible under a UV lamp, where the green solution of Sensor 1 became orange–red upon titration with CaDPA (Figure 2 C). In this case, a color change can be identified by the naked eye, even at a CaDPA concentration as low as 1 μM, making the naked-eye detection of low concentrations of CaDPA possible.

The time-dependent fluorescence response of Sensor 1 to 10 μM CaDPA was monitored at 616 nm with an excitation wavelength of 270 nm (Figure 3). The curve showed a rapid enhancement of the fluorescence intensity in the first 10 s followed by a slower increase over the next 20 s, which revealed that the reaction is complete within 30 s, thus enabling a rapid detection of *B. anthracis* spores.

An important practical challenge for europium-based nanoparticle sensors is how to decrease the interference resulting from the nonselective binding of aromatic ligands to Eu^{III}. Reducing this interference would improve the selectivity towards *B. anthracis* spores. With this in mind, the fluorescence enhancement effects of aromatic ligands such as benzoic acid, *m*-phthalic acid and *o*-phthalic acid on Sensor 1 were investigated. As demonstrated in Figure 4 A, only CaDPA induced a prominent fluorescence enhancement, whereas only very weak fluorescence changes were observed for aromatic ligands even at a concentration as high as 1 mM

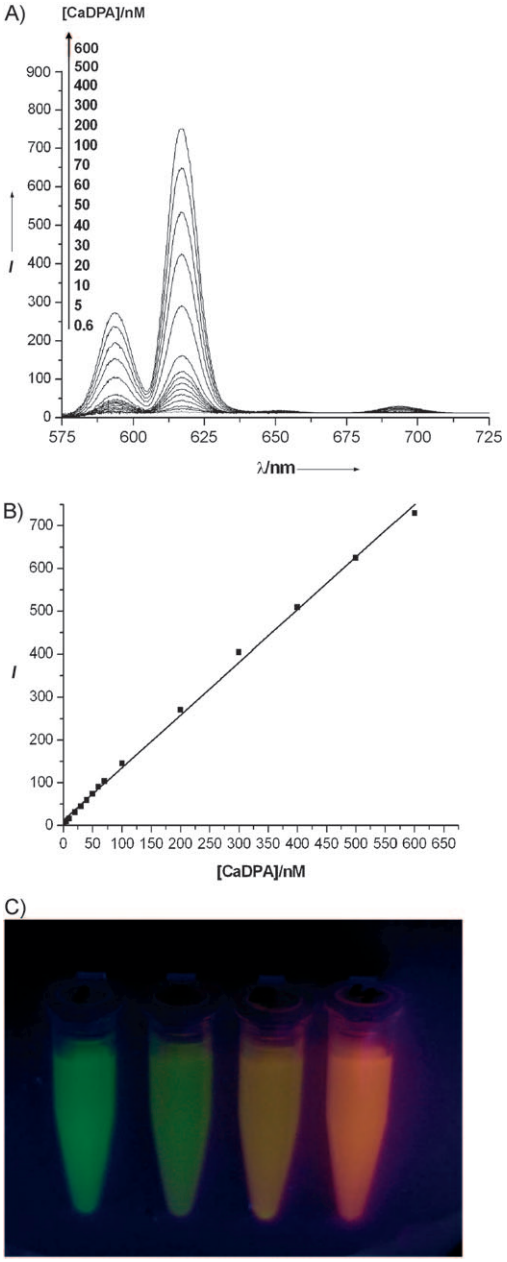

Figure 2. A) Fluorescence response of Sensor 1 (Eu^{III} content: 10 μM) upon addition of different concentrations of CaDPA at pH 6.5. B) The fluorescence intensity at 616 nm of Sensor 1 as a function of CaDPA concentration. C) Visual fluorescence color changes of Sensor 1 (Eu^{III} content: 120 μM) upon addition of different concentrations of CaDPA (from left to right: 0, 25 μM, 50 μM, 100 μM).

(Supporting Information Figure S5). In a control experiment, we also tested the fluorescence enhancement effects of the above aromatic ligands on the terbium-based nanoparticle sensor, which is described in the Experimental Section under same conditions. The results indicated that the presence of *o*-phthalic acid had a modest interfering effect on CaDPA sensing with the terbium sensor (Figure 4 B). Such an improvement in the selectivity over the terbium-based sensors can be rationalized as follows. As mentioned above, Eu^{III} excited states can couple more efficiently with the high-

 © 2009 Wiley-VCH Verlag GmbH & Co. KGaA, Weinheim

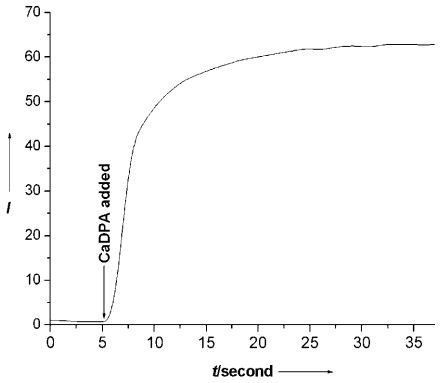

Figure 3. Plot of fluorescence intensity versus time for Sensor 1 at 616 nm upon addition of 10 μM CaDPA at pH 6.5.

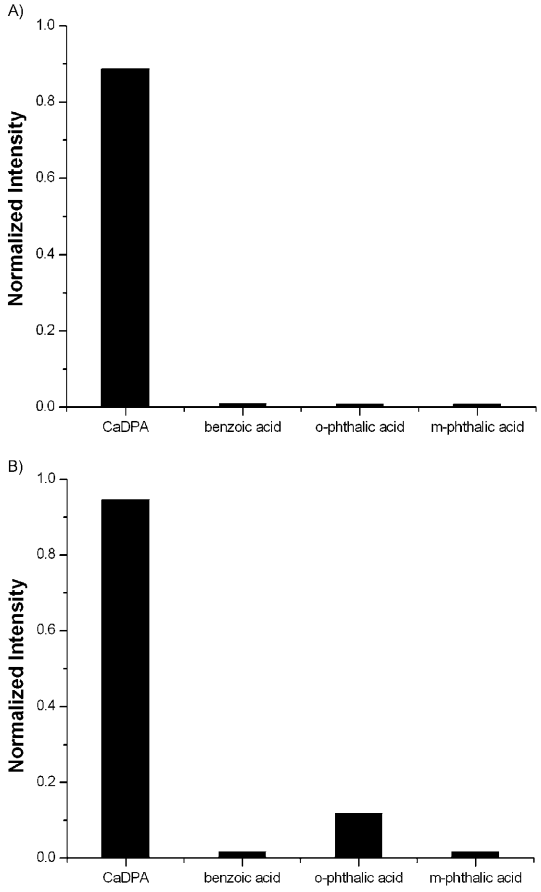

Figure 4. Plot of fluorescence intensity of A) the europium-based nanoparticle sensor (Sensor 1) and B) the terbium-based sensor with CaDPA, benzoic acid, *m*-phthalic acid and *o*-phthalic acid (from left to right, concentration: 1 mM; monitored at the maximum fluorescence intensity).

frequency OH oscillators of water molecules in comparison with Tb^{III}, which means that water molecules more efficiently quench the Eu^{III} emission than the Tb^{III} emission through OH vibrational deactivation. Many aromatic ligands such as benzoic acid, *m*-phthalic acid, and *o*-phthalic acid, can not displace completely all three coordinating water molecules from the Eu^{III} or Tb^{III} center. The residual coordinating water molecule can still efficiently quench the Eu^{III} emission of Sensor 1, thus decreasing false-positive results arising from nonselective binding of aromatic compounds. However, the residual coordinating water molecule is less efficient at quenching the Tb^{III} emission (as evidenced by Figure S5B in the Supporting Information).

The exclusion of second-order scattering interference in the maximum fluorescence intensity is another important advantage of Sensor 1 over terbium-based nanoparticle sensors (Supporting Information Figure S6A). In the case of terbium-based nanoparticle sensors, the most efficient terbium emission was achieved upon excitation at 270 nm. However, the strong interference from the second-order scattering peak at 540 nm makes it difficult to directly observe the change in the maximum terbium emission intensity at 544 nm (Figure S6B). To decrease such interference, 278 nm is often used as the excitation wavelength, which hence lowers the sensitivity of terbium-based nanoparticle sensors toward *B. anthracis* spores.[6]

In summary, we have demonstrated for the first time, the realization of a europium-based nanoparticle sensor for the rapid and ultrasensitive detection of *B. anthracis* spores in aqueous solution. In comparison with reported terbium-based sensors, the sensitivity of the europium-based sensor toward CaDPA, an anthrax biomarker, is higher (LOD = 0.2 nM), and has a remarkable selectivity over aromatic ligands in aqueous solution. A particularly attractive feature of this sensor is the combining of the properties of the europium complex and the organic dye-doped silica nanoparticle, which makes the fabrication of CaDPA responsive devices for practical applications possible. These studies are in progress.

Experimental Section

Synthesis of FITC-doped silica nanoparticles: FITC was firstly linked to the coupling agent APTES by a reaction of FITC (0.5 mg) and APTES (50 μL) in 1-hexanol (2.5 mL) of under N_2 protection. Next, 0.2 mL of the resulting APTES–FITC conjugates was added to the water/oil (W/O) microemulsion solution containing cyclohexane (7.5 mL), 1-hexanol (1.6 mL), Triton X-100 (1.77 g), and deionized water (480 μL), and stirred for 15 min. TEOS (50 μL) was then added. After stirring for another 30 min, the hydrolysis of TEOS and FITC–APTES was initiated by the addition of NH_4OH (60 μL), and the mixture was stirred for 24 h. The final surface layer incorporating primary amines was formed by adding APTES (50 μL) and stirring for 24 h. Finally, the as-prepared FITC-doped silica nanoparticles were centrifuged and washed four times with ethanol and three times with deionized water.

Synthesis of EDTA dianhydride: Ethylenediamine tetraacetic acid (EDTA, 20 g) was placed in a 250 mL three-neck flask equipped with a condenser, a magnetic stirrer and a heating mantle. Acetic anhydride (37.8 mL) and pyridine (25.5 mL) were added to the flask, and the mixture was stirred for 24 h at 63 °C. The resulting anhydride was collected by filtration, washed thoroughly with acetic anhydride and dry diethyl ether. The cream-colored powder was then freeze-dried.

Sensor 1: FITC-doped silica nanoparticles (100 mg) were redispersed by sonication in bicarbonate buffer (20 mL; 0.1M) at pH 9.6. EDTA dianhydride (300 mg) was added. After stirring for 2 h, the as-prepared nanoparticles were separated by centrifuging and then washed four times with bicarbonate buffer and two times with deionized water (Supporting Information Figure S7). Subsequently,

 © 2009 Wiley-VCH Verlag GmbH & Co. KGaA, Weinheim

the as-prepared nanoparticles were redispersed in aqueous solution of $EuCl_3$ (20 mL; 0.01M) by sonication and stirred for 5 h. Finally, the products were collected by centrifuging and washed with deionized water several times to remove residual $EuCl_3$. In the case of CaDPA sensing, the concentration of Sensor 1 is calculated by using the content of europium unless otherwise specified. In a control experiment, the terbium-based sensor was prepared using the similar strategy for comparison, however, to avoid strong interference of second-ordering scattering in the maximum fluorescence intensity,[6] FITC-doped silica nanoparticle was absent in this case and the 278 nm excitation wavelength was used.

Characterization: The nanoparticle size was examined using JEOL 2000-FX transmission electron microscopy (TEM). UV/Vis spectra were recorded on a VARIAN CARY 50 UV/Vis spectrophotometer. Fluorescence spectra were obtained using a SHIMADZU RF-5301PC spectrofluorometer (after filtration with a CB565 filter). Fluorescence lifetime data were measured with a Lecroy Wave Runner 6100 digital oscilloscope (1 GHz) using a 266 nm laser (pulse width of 4 ns) as the excitation source (Continuum Sunlite OPO). NMR spectroscopy experiments were performed on a Varian Infinity-plus 400 spectrometer operating at a magnetic field strength of 9.4 T. A Chemagnetics 7.5 mm triple-resonance magic-angle spinning (MAS) probe was used to acquire all the spectra at a spinning rate of 4 kHz.

Received: August 27, 2008
Published online: December 3, 2008

Keywords: anthrax · europium · fluorescence · nanoparticles · sensors

[1] a) M. Enserink, *Science* **2001**, *294*, 490 – 491; b) D. L. Rosen, C. Sharpless, L. B. McGown, *Anal. Chem.* **1997**, *69*, 1082 – 1085; c) P. M. Pellegrino, N. F. Fell, Jr., D. L. Rosen, J. B. Gillespie, *Anal. Chem.* **1998**, *70*, 1755 – 1760; d) X. Zhang, J. Zhao, A. V. Whitney, J. W. Elam, R. P. Van Duyne, *J. Am. Chem. Soc.* **2006**, *128*, 10304 – 10309; e) D. D. Evanoff, Jr., J. Heckel, T. P. Caldwell, K. A. Christensen, G. Chumanov, *J. Am. Chem. Soc.* **2006**, *128*, 12618 – 12619; f) M. L. Cable, J. P. Kirby, K. Soarasaenee, H. B. Gray, A. Ponce, *J. Am. Chem. Soc.* **2007**, *129*, 1474 – 1475.

[2] a) D. King, V. Luna, A. Cannons, J. Cattani, P. Amusi, *J. Clin. Microbiol.* **2003**, *41*, 3454 – 3455; b) W. Hurtle, E. Bode, D. A. Kulesh, R. S. Kaplan, J. Garrison, D, Bridge, M. House, M. S. Frye, B. Loveless, D. Norwood, *J. Clin. Microbiol.* **2004**, *42*, 179 – 185; c) B. H. Zhang, H. S. Wang, L. H. Lu, K. L. Ai, G. Zhang, X. L. Chen, *Adv. Funct. Mater.* **2008**, *18*, 2348 – 2355; d) L. H. Lu, A. Eychmüller, *Acc. Chem. Res.* **2008**, *41*, 244 – 253.

[3] D. R. Walt, D. R. Franz, *Anal. Chem.* **2000**, *72*, 738A – 746A.

[4] a) K. Hanaoka, Ki. Kikuchi, H. Kojima, Y. Urano, T. Nagano, *Angew. Chem.* **2003**, *115*, 3104 – 3107; *Angew. Chem. Int. Ed.* **2003**, *42*, 2996 – 2999; b) B. I. Ipe, K. Yoosaf, K. G. Thomas, *J. Am. Chem. Soc.* **2006**, *128*, 1907 – 1913; c) R. F. H. Viguier, A. N. Hulme, *J. Am. Chem. Soc.* **2006**, *128*, 11370 – 11371; d) J. Massue, S. J. Quinn, T. Gunnlaugsson, *J. Am. Chem. Soc.* **2008**, *130*, 6900 – 6901.

[5] a) H. Tsukube, S. Shinoda, *Chem. Rev.* **2002**, *102*, 2389 – 2404; b) S. Pandya, J. Yu, D. Parker, *Dalton Trans.* **2006**, 2757 – 2766; c) K. R. Kupcho, D. K. Stafslien, T. DeRosier, T. M. Hallis, M. S. Ozers, K. W. Vogel, *J. Am. Chem. Soc.* **2007**, *129*, 13372 – 13373; d) K. Hanaoka, K. Kikuchi, S. Kobayashi, T. Nagano, *J. Am. Chem. Soc.* **2007**, *129*, 13502 – 13509.

[6] W. J. Rieter, K. M. L. Taylor, W. B. Lin, *J. Am. Chem. Soc.* **2007**, *129*, 9852 – 9853.

[7] a) A. Beeby, I. M. Clarkson, R. S. Dickins, S. Faulkner, D. Parker, L. Royle, A. S. de Sousa, J. A. G. Williams, M. Woods, *J. Chem. Soc. Perkin Trans. 2* **1999**, 493 – 503; b) M. Xiao, P. R. Selvin, *J. Am. Chem. Soc.* **2001**, *123*, 7067 – 7073; c) D. Parker, R. S. Dickins, H. Puschmann, C. Crossland, J. A. K. Howard, *Chem. Rev.* **2002**, *102*, 1977 – 2010.

[8] a) X. Zhao, R. P. Bagwe, W. H. Tan, *Adv. Mater.* **2004**, *16*, 173 – 176; b) A. Burns, H. Ow, U. Wiesner, *Chem. Soc. Rev.* **2006**, *35*, 1028 – 1042.

[9] C. H. Paik, M. A. Ebbert, P. R. Murphy, C. R. Lassman, R. C. Reba, W. C. Eckelman, K. Y. Pak, J. Powe, Z. Steplewski, H. Koprowski, *J. Nucl. Med.* **1983**, *24*, 1158 – 1163.

[10] a) T. Gunnlaugsson, J. P. Leonard, *Chem. Commun.* **2003**, 2424 – 2425; b) M. S. Tremblay, Q. Zhu, A. A. Dyer, M. Halim, S. Jockusch, N. J. Turro, D. Sames, *Org. Lett.* **2006**, *8*, 2723 – 2726; c) S. Comby, D. Imbert, C. Vandevyver, J. C. G. Bünzil, *Chem. Eur. J.* **2007**, *13*, 936 – 944.

 © 2009 Wiley-VCH Verlag GmbH & Co. KGaA, Weinheim